



HAL
open science

Sub-25 ps timing measurements with 10 x 10 cm² PICOSEC Micromegas detectors

M. Lisowska, J. Bortfeldt, F. Brunbauer, G. Fanourakis, K.J. Floethner, M. Gallinaro, F. Garcia, I. Giomataris, T. Gustavsson, F.J. Iguaz, et al.

► **To cite this version:**

M. Lisowska, J. Bortfeldt, F. Brunbauer, G. Fanourakis, K.J. Floethner, et al.. Sub-25 ps timing measurements with 10 x 10 cm² PICOSEC Micromegas detectors. Nuclear Instruments and Methods in Physics Research Section A: Accelerators, Spectrometers, Detectors and Associated Equipment, 2022, pp.167687. 10.1016/j.nima.2022.167687 . cea-03844611

HAL Id: cea-03844611

<https://cea.hal.science/cea-03844611>

Submitted on 8 Nov 2022

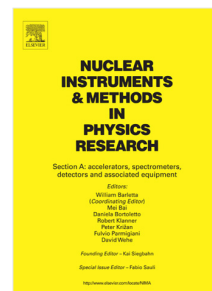
HAL is a multi-disciplinary open access archive for the deposit and dissemination of scientific research documents, whether they are published or not. The documents may come from teaching and research institutions in France or abroad, or from public or private research centers.

L'archive ouverte pluridisciplinaire **HAL**, est destinée au dépôt et à la diffusion de documents scientifiques de niveau recherche, publiés ou non, émanant des établissements d'enseignement et de recherche français ou étrangers, des laboratoires publics ou privés.

Journal Pre-proof

Sub-25 ps timing measurements with $10 \times 10 \text{ cm}^2$ PICOSEC Micromegas detectors

M. Lisowska, J. Bortfeldt, F. Brunbauer, G. Fanourakis, K.J. Floethner, M. Gallinaro, F. Garcia, I. Giomataris, T. Gustavsson, F.J. Iguaz, D. Janssens, A. Kallitsopoulou, M. Kovacic, P. Legou, J. Liu, M. Lupberger, I. Maniatis, Y. Meng, H. Muller, E. Oliveri, G. Orlandini, T. Papaevangelou, M. Pomorski, L. Ropelewski, D. Sampsonidis, L. Scharenberg, T. Schneider, L. Sohl, M. van Stenis, Y. Tsipolitis, S.E. Tzamarias, A. Utrobicic, R. Veenhof, X. Wang, S. White, Z. Zhang, Y. Zhou



PII: S0168-9002(22)00979-2
DOI: <https://doi.org/10.1016/j.nima.2022.167687>
Reference: NIMA 167687

To appear in: *Nuclear Inst. and Methods in Physics Research, A*

Received date: 31 August 2022
Revised date: 17 October 2022
Accepted date: 19 October 2022

Please cite this article as: M. Lisowska, J. Bortfeldt, F. Brunbauer et al., Sub-25 ps timing measurements with $10 \times 10 \text{ cm}^2$ PICOSEC Micromegas detectors, *Nuclear Inst. and Methods in Physics Research, A* (2022), doi: <https://doi.org/10.1016/j.nima.2022.167687>.

This is a PDF file of an article that has undergone enhancements after acceptance, such as the addition of a cover page and metadata, and formatting for readability, but it is not yet the definitive version of record. This version will undergo additional copyediting, typesetting and review before it is published in its final form, but we are providing this version to give early visibility of the article. Please note that, during the production process, errors may be discovered which could affect the content, and all legal disclaimers that apply to the journal pertain.

© 2022 The Author(s). Published by Elsevier B.V. This is an open access article under the CC BY license (<http://creativecommons.org/licenses/by/4.0/>).

Sub-25 ps timing measurements with $10 \times 10 \text{ cm}^2$ PICOSEC Micromegas detectors

M. Lisowska^{a,b,*}, J. Bortfeldt^c, F. Brunbauer^a, G. Fanourakis^d, K. J. Floethner^{a,e}, M. Gallinaro^f, F. Garcia^g, I. Giomataris^h, T. Gustavssonⁱ, F.J. Iguaz^h, D. Janssens^{a,j,k}, A. Kallitsopoulou^h, M. Kovacic^l, P. Legou^h, J. Liu^m, M. Lupberger^{e,n}, I. Maniatis^{a,o}, Y. Meng^m, H. Muller^{a,n}, E. Oliveri^a, G. Orlandini^{a,p}, T. Papaevangelou^h, M. Pomorski^q, L. Ropelewski^a, D. Sampsonidis^{o,r}, L. Scharenberg^{a,n}, T. Schneider^a, L. Sohl^h, M. van Stenis^a, Y. Tsiopolitis^s, S.E. Tzamarias^{o,r}, A. Utrobicic^a, R. Veenhof^{a,t}, X. Wang^m, S. White^{a,u}, Z. Zhang^m, Y. Zhou^m

^aEuropean Organization for Nuclear Research (CERN), CH-1211, Geneva 23, Switzerland,

^bUniversité Paris-Saclay, F-91191 Gif-sur-Yvette, France,

^cDepartment for Medical Physics, Ludwig Maximilian University of Munich, Am Coulombwall 1, 85748 Garching, Germany,

^dInstitute of Nuclear and Particle Physics, NCSR Demokritos, GR-15341 Agia Paraskevi, Attiki, Greece,

^eHelmholtz-Institut für Strahlen- und Kernphysik, University of Bonn, Nußallee 14–16, 53115 Bonn, Germany,

^fLaboratório de Instrumentação e Física Experimental de Partículas, Lisbon, Portugal,

^gHelsinki Institute of Physics, University of Helsinki, FI-00014 Helsinki, Finland,

^hIRFU, CEA, Université Paris-Saclay, F-91191 Gif-sur-Yvette, France,

ⁱLIDYL, CEA, CNRS, Université Paris-Saclay, F-91191 Gif-sur-Yvette, France,

^jInter-University Institute for High Energies (IIHE), Belgium,

^kVrije Universiteit Brussel, Pleinlaan 2, 1050 Brussels, Belgium,

^lFaculty of Electrical Engineering and Computing, University of Zagreb, 10000 Zagreb, Croatia,

^mState Key Laboratory of Particle Detection and Electronics, University of Science and Technology of China, Hefei 230026, China,

ⁿPhysikalisches Institut, University of Bonn, Nußallee 12, 53115 Bonn, Germany,

^oDepartment of Physics, Aristotle University of Thessaloniki, University Campus, GR-54124, Thessaloniki, Greece,

^pFriedrich-Alexander-Universität Erlangen-Nürnberg, Schloßplatz 4, 91054 Erlangen, Germany,

^qCEA-LIST, Diamond Sensors Laboratory, CEA Saclay, F-91191 Gif-sur-Yvette, France,

*Corresponding author.

Email address: marta.lisowska@cern.ch (M. Lisowska)

^rCenter for Interdisciplinary Research and Innovation (CIRI-AUTH), Thessaloniki
57001, Greece,
^sNational Technical University of Athens, Athens, Greece,
^tBursa Uludağ University, Görükle Kampusu, 16059 Niüfer/Bursa, Turkey,
^uUniversity of Virginia, USA,

Abstract

The PICOSEC Micromegas detector is a precise timing gaseous detector based on a Cherenkov radiator coupled to a semi-transparent photocathode and a Micromegas amplifying structure. First single-pad prototypes demonstrated a time resolution below $\sigma = 25$ ps, however, to make the concept appropriate to physics applications, several developments are required. The objective of this work was to achieve an equivalent time resolution for a 10×10 cm² area PICOSEC Micromegas detector. The prototype was designed, produced and tested in the laboratory and successfully operated with a 80 GeV/c muon beam. Preliminary results for this device equipped with a CsI photocathode demonstrated a time resolution below $\sigma = 25$ ps for all measured pads. The time resolution was reduced to be below $\sigma = 18$ ps by decreasing the drift gap to 180 μ m and using dedicated RF amplifier cards as new electronics. The excellent timing performance of the single-channel proof of concept was not only transferred to the 100-channel prototype, but even improved, making the PICOSEC Micromegas detector more suitable for large-area experiments in need of detectors with high time resolutions.

Keywords: Gaseous detectors, Micromegas, Multipad, Timing resolution

1. Introduction

The challenges of future High Energy Physics experiments, including high-pile-up environments expected in the High-Luminosity Large Hadron Collider (HL-LHC), have aroused intense interest in the development of technologies for detectors with high time resolution. A time resolution of tens of picoseconds, stable long-term operation and a large area coverage are key requirements that these devices must fulfil to be applicable in demanding environments such as the HL-LHC. The first PICOSEC Micromegas (MM) prototype indicated how precise time resolution can be achieved with a single-channel gaseous detector with an active area of 1 cm in diameter [1]. Although the detector's proof of concept demonstrated a $\sigma = 25$ ps time resolution, this excellent timing performance has never been transferred to a 100-channel device. The objective of this work was to achieve an equivalent time resolution for the 100-channel PICOSEC MM detector with an active area of 10×10 cm².

In Section 2, the PICOSEC MM detection concept is outlined. Section 3 is a description of the 10×10 cm² area PICOSEC MM detector design and production. In Section 4, the electronics dedicated to the 100 channels detector, including custom-made amplifiers and SAMPIC digitizer, are explained. The results from timing measurements obtained for the 10×10 cm² multi-pad detectors are presented and discussed in Section 5. Section 6 gives an outlook of the PICOSEC MM detector robustness aspects that need to be implemented, including resistive MM and robust photocathodes. Section 7 is a summary of the conclusions drawn from this paper.

25 **2. PICOSEC Micromegas detection concept**

26 Within the PICOSEC MM collaboration, a gaseous detector that aims at
27 reaching a time resolution of tens of picoseconds is being developed [1]. The
28 PICOSEC MM detection concept is presented in Fig. 1. A charged particle
29 passing through a Cherenkov radiator (3 mm thick MgF_2 crystal) creates a
30 cone of UV photons that are converted into photoelectrons on the photo-
31 cathode. The baseline converter of the UV photons into the photoelectrons
32 for the PICOSEC MM detector is a 18 nm thick Cesium Iodide (CsI) semi-
33 transparent photocathode. Following the extraction of the primary electrons
34 from the photocathode, a high electric field in the drift gap leads to succes-
35 sive ionisations by the primary electrons and thus a pre-amplification. After
36 passing through the MM mesh, the electrons are additionally multiplied in
37 the amplification gap. Both regions are filled with a flammable gas mixture
38 of 80% neon, 10% CF_4 and 10% ethane. The amplified electrons induce a
39 signal on the anode which is passed through an amplifier and read-out by a
40 digitizer. A typical PICOSEC MM waveform displaying a fast electron peak
41 and a slow ion tail is presented in Fig. 2. The rising edge of the electron
42 peak is used to calculate the time of arrival.

43 The first single-pad prototypes demonstrated time resolution below $\sigma =$
44 25 ps [1]. To make the concept appropriate to physics applications, several
45 developments are required. Since the objective is to build a tileable multi-
46 channel detector modules for large area coverage, the project progressed from
47 a single-pad prototype [1] to a 19-channels device [2] before the current 100-
48 channel module [3] which is the main subject of this study. The active area
49 of the detector changed from 1 cm to 3.6 cm diameter circle between single-

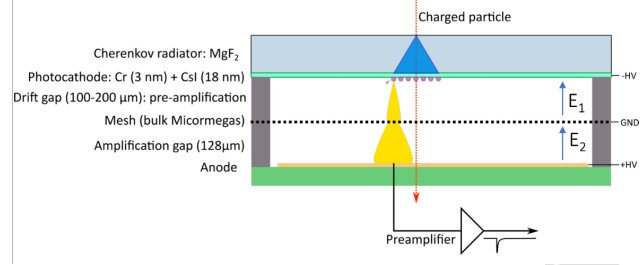


Figure 1: Schematic representation of the PICOSEC detection concept. A charged particle passing through a Cherenkov radiator creates UV photons that are converted into primary electrons on a photocathode, pre-amplified in the drift gap and multiplied in the amplification gap [3].

50 and multi-pad prototypes and it was scaled up to 10×10 cm² for the 100-
 51 channel module, increasing the surface almost 10 times in comparison to
 52 the 19-channels device. The evolution of the PICOSEC MM detectors is
 53 presented in Fig. 3. The detector's mechanics, electronics and robustness
 54 are some of the developments towards applicable device that are presented
 55 in this work.

56 **3. Design and production of the 10×10 cm² area PICOSEC Mi-** 57 **cromegas detector**

58 The PICOSEC MM detectors consist of a printed circuit board (PCB) on
 59 top of which a woven mesh of 18 μm thick steel wires is stretched over pillars
 60 and a coverlay (Pyradox PC1025) frame. The thickness of the amplification
 61 gap is defined by the height of the bottom coverlay and the pillars and chosen
 62 to be 128 μm. The thickness of the drift gap is defined by the spacer placed
 63 on top of the mesh stretching frame which in the standard configuration is

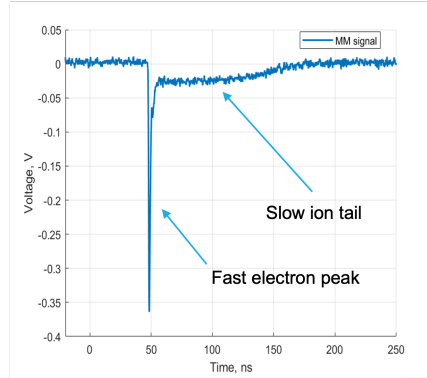


Figure 2: A typical PICOSEC MM waveform displaying a fast electron peak and a slow ion tail [3].

64 200 μm .

65 The first PICOSEC MM multipad prototype was a 19-channels detector
 66 with a circular-shaped active area of 3.6 cm in diameter and a PCB made
 67 of a 3.2 mm thick FR4 plate [2]. Preliminary measurements of the detector
 68 flatness showed deformations in the active area in the range of 30 μm that
 69 caused a non-uniform drift gap and resulted in a non-uniform response of
 70 the device. The deformations were introduced by mechanical stress on the
 71 PCB due to fixing it to the detector flange as well as non-flatness of the PCB
 72 because of the forces originating from stretching the mesh on top of it. For
 73 scaling-up this prototype, the problem of the deformations was anticipated
 74 to be more pronounced for the larger active areas. The requirement for
 75 the $10 \times 10 \text{ cm}^2$ module was to obtain precise mechanical parts to preserve
 76 uniform thickness of the drift gap.

77 In order to improve the flatness of the active area, the necessary steps
 78 were to decouple the PCB from the flange by using a second board called

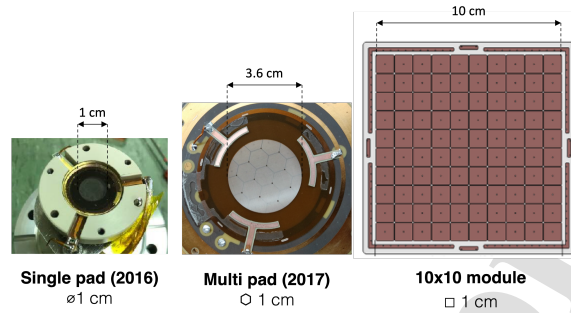


Figure 3: The evolution of thw PICOSEC MM detectors. From left to right: a single-pad prototype [1], a 19-channels device [2], the 100-channel module [3]. Note that the figures are not in scale.

79 outer PCB and design a more rigid MM PCB [3, 4], as can be seen in Fig.
 80 4. To avoid the mechanical connection of the MM PCB to the housing, a
 81 new design was made which includes a 6 mm thick outer PCB screwed to the
 82 aluminum housing. The outer PCB was connected with the MM PCB with
 83 spring-loaded pins. To choose more rigid MM PCB material and its proper
 84 thickness, structural simulations of the board deformations under mesh ten-
 85 sion were performed using open-source tools: FreeCAD, Gmsh and CalculiX
 86 [5]. Based on the experience from the first 19-channels prototype, the main
 87 objective for the $10 \times 10 \text{ cm}^2$ module was to minimise the deformations below
 88 $10 \text{ }\mu\text{m}$ throughout the whole active area. The calculations included analysis
 89 of how the mesh tension and contact pressure influence the planarity. Sim-
 90 ulations suggested that a big gain in planarity can be achieved by a change
 91 of the material and only a small increase in the ceramics thickness, as can
 92 be seen in Table A.1. The influence of the mesh tension on the planarity of
 93 a 4 mm thick ceramic board resulted in maximum calculated displacement

94 in the active area of around $4\ \mu\text{m}$, which is presented in Fig. 5. The final
 95 design of the MM PCB, shown in Fig. 6, consists of a 4.85 mm thick hybrid
 96 ceramic-FR4 board instead of a 3 mm thick pure FR4 one.

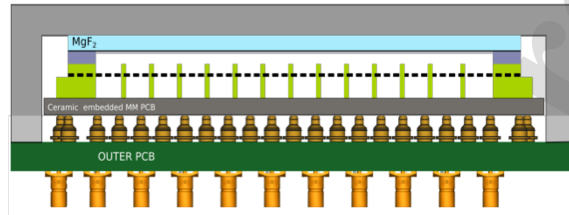


Figure 4: A new PICOSEC MM detector design consisting of 2 separate PCBs: an outer board screwed to the aluminum housing and a more rigid hybrid ceramic-FR4 MM board. The outer PCB was connected with the MM PCB with spring-loaded pins [3].

97 The production of the hybrid ceramic-FR4 board was monitored with
 98 planarity measurements using a Keyence 3D microscope from the beginning
 99 of the process [6]. The analysis of the board before the bulking showed that
 100 its planarity was within the specifications, as can be seen in Fig. 7. The
 101 100 channels PICOSEC MM detector with flatness deformations below $10\ \mu\text{m}$
 102 was successfully produced, preserving uniform thickness of the drift gap.

103 4. Electronics dedicated to the 100 channels detector

104 4.1. Custom-made amplifiers

105 The primary used electronics for amplifying signals induced on the anode
 106 was the CIVIDEC C2 [7], a low-noise amplifier with an analog bandwidth of 2
 107 GHz, a gain of 40 dB, and an oscilloscope for digitising waveforms. However,
 108 the use of 100 CIVIDECs is highly impractical when it comes to scaling to

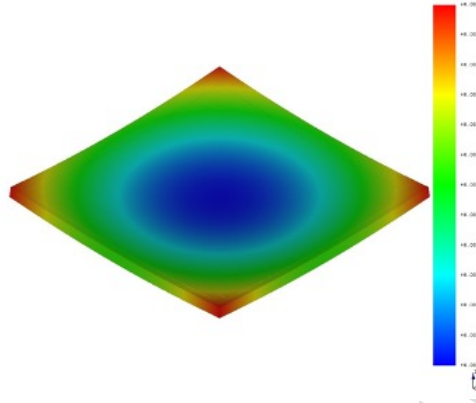


Figure 5: A simulation of the mesh tension influence on the planarity. For a 4 mm thick ceramic PCB, a maximum displacement in the active area of around 4 μm was calculated [4].

109 multiple channels detectors. Therefore, several different types of custom-
 110 made amplifiers are being developed. A promising solution are RF pulse
 111 amplifier cards optimised for the PICOSEC. The design was based on the
 112 RF pulse amplifier for CVD diamond particle detectors [8] and modified with
 113 a spark protection up to 350 V, a bandwidth of 650 MHz, a gain of 38 dB and
 114 a power consumption of 75 mW per channel [9]. The results obtained for the
 115 measurements performed with these amplifiers are presented and discussed
 116 in Subsection 5.4.

117 4.2. SAMPIC digitizer

118 After the amplification, the signal needs to be read-out. The baseline
 119 digitizer for the PICOSEC MM detector is an oscilloscope with 10 GS/s
 120 sampling frequency. Again, the use of 100 oscilloscope channels is highly
 121 impractical when it comes to scaling to multiple channels detectors. There-

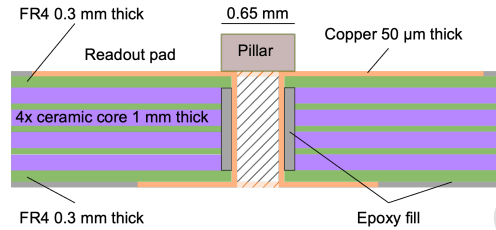


Figure 6: The final design of the MM PCB consisting of a 4,85 mm thick hybrid ceramic-FR4 board. The anode read-out pads are connected to the back side pads through vias that are plated and filled with conductive epoxy [3].

122 fore, the SAMPIC waveform TDC digitizer [10] is currently being tested.
 123 During the last beam campaigns, a 64 channel SAMPIC was tested, while a
 124 128 channel device is being implemented for reading out the PICOSEC MM
 125 modules. While the maximum available sampling frequency of currently used
 126 SAMPIC modules is limited to 8.5 GS/s, this appears to be sufficient to pre-
 127 serve the timing precision of the PICOSEC MM detectors. The principle
 128 of the complete readout chain was proven for the first time by a successful
 129 readout of 50 multipad PICOSEC channels.

130 5. Timing measurements of the $10 \times 10 \text{ cm}^2$ area multipad PICOSEC

131 5.1. Experimental setup

132 The 100 channels PICOSEC MM detectors were tested in the laboratory
 133 and successfully operated during test beam campaigns. The main purpose of
 134 the campaigns was to measure timing resolution of the prototypes assembled
 135 in different configurations. The measurements were performed at the CERN
 136 SPS H4 beam line with a 80 GeV/c muon beam. The main part of the

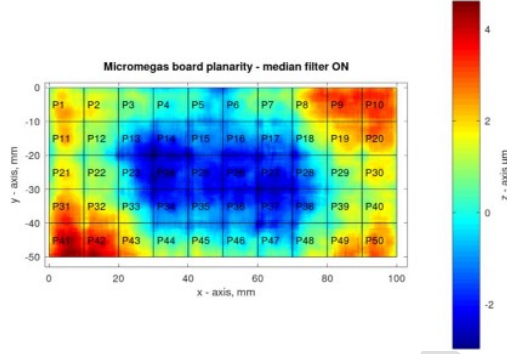


Figure 7: Planarity measurements of the top half of the PICOSEC Micromegas detector showing flatness deformations below $10 \mu\text{m}$ [6].

137 test setup consisted of a beam telescope with triggering, timing and tracking
 138 capabilities. An example of a telescope configuration is presented in Fig.
 139 8. The precise tracking of the particles was done using triple-GEMs with
 140 a spatial resolution below $80 \mu\text{m}$. Multiple micro-channel plate photomulti-
 141 plier tubes (MCP-PMTs) were used as timing reference and data acquisition
 142 (DAQ) trigger. The telescope was built in such a way that it could perform
 143 tests of several devices at the same time.

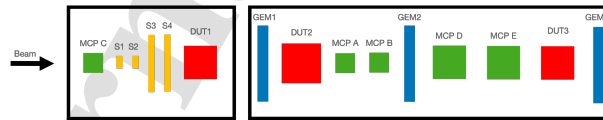


Figure 8: An example of a telescope configuration consisting of GEM detectors for precise tracking (in blue), MCP-PMTs for timing reference and DAQ (in green) and devices under test (in red). DAQ could also be done by using a coincidence of four scintillators (in yellow).

144 *5.2. Time resolution analysis procedure*

145 To properly quantify the timing precision of the PICOSEC detectors,
146 a reference device with better timing precision was required. In the work
147 presented here, an MCP-PMT (R3809U-50 Hamamatsu) with a uniform re-
148 sponse in the area of 11 mm in diameter was used as a timing reference of
149 the PICOSEC prototype. The devices were spatially aligned with respect to
150 each other, so when muons passed through them, signals on both detectors
151 were induced. In the analysis, a sigmoid functions were fitted to the lead-
152 ing edges of the electron peaks giving the positions of the signals in time
153 at the 20% Constant Fraction (CF) [3]. The signal arrival time (SAT) was
154 defined as a difference between PICOSEC detector and reference device tim-
155 ing marks. The time resolution of the detector was calculated as a standard
156 deviation of the SAT distribution. The contribution of the MCP-PMT was
157 not subtracted from the time resolution of the PICOSEC detector for all the
158 measurements presented in this work.

159 *5.3. Time response of the multipad PICOSEC in the standard configuration*

160 First test beam measurements of the multipad PICOSEC were performed
161 using the "standard" configuration of the prototype: non-resistive detector
162 with 220 μm drift gap, 3 mm MgF_2 radiator with CsI photocathode and
163 the CIVIDEC amplifier. The aim of the experiment was to obtain timing
164 resolution when signals were fully contained within the center of individual
165 pads within $5 \times 5 \text{ mm}^2$ area. Preliminary results show uniform time resolution
166 of $\sigma = 25 \text{ ps}$ or below for all measured pads [3], confirming that the excellent
167 timing performance can be transferred from a single-pad prototype to a 100-
168 channel module. An example of a SAT distribution of one channel with time

169 resolution, obtained by using the standard deviation, is shown in Fig. 9 and
 170 the results from all tested pads are summarised in Table A.2.

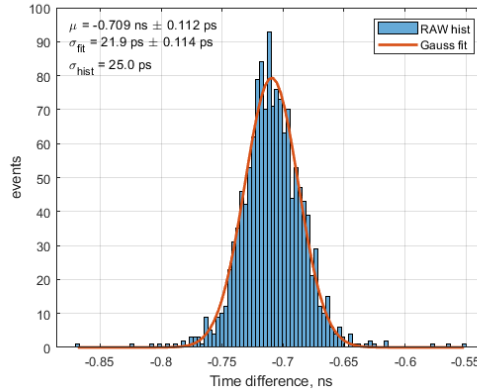


Figure 9: SAT distribution of one channel of the multipad PICOSEC while performing test beam measurements in the "standard" configuration of the detector. The voltage on the cathode was 500 V and on the anode 275 V. The histogram consist of the data after implementing a geometrical cut which was a 4 mm diameter circle made in the center of the pad. Time resolution of the measured channel was $\sigma = 25.0$ ps.

171 When a particle hits the detector in between the pads or in the corner of
 172 the active area and the induced signal is not fully contained inside a single
 173 channel, the timing capabilities of that channel are reduced [2]. Therefore,
 174 sharing of the signal between 4 neighbouring pads was studied in order to test
 175 the possibility of timing reconstruction. For this test the same "standard"
 176 configuration of the multipad PICOSEC was used. The measurement was
 177 performed using the MCP-PMT centered in the cross between 4 channels
 178 of the detector and the signals from both devices were sufficiently collected
 179 during one run. The experiment confirmed that timing information can be

180 reconstructed when the signal is shared between pads. The obtained time
181 resolution was $\sigma = 30.0$ ps [11, 12].

182 *5.4. Time response of the multipad PICOSEC with the custom-made ampli-*
183 *fier cards and the reduced drift gap*

184 First test beam measurements with custom-made RF pulse amplifiers
185 optimised for the PICOSEC MM detectors were done as a next step towards
186 the improvement of the time response of the device. Except for the new
187 amplifiers, the detector was in the "standard" configuration. Results from
188 the signals fully contained within the center of individual pads within 5×5
189 mm^2 area confirmed the improvement of the time resolution. This may be
190 attributed to the lower bandwidth, which suppress the noise components,
191 and better impedance matching of the new amplifiers to the detector in
192 comparison to the CIVIDEC electronics. The time resolution obtained for
193 these measurements was below $\sigma = 22$ ps for all tested pads [9]. An example
194 of a SAT distribution of one channel is shown in Fig. 10 and results from all
195 measured pads are summarised in Table A.3.

196 A final adjustment towards improving the time resolution of the PI-
197 COSEC MM detector was the reduction of the drift gap. The time resolution
198 depends on the SAT which can be reduced by employing a higher drift field
199 [13]. The higher drift field can be achieved by applying higher voltages on
200 the electrodes, however, when too much charge is produced, the operation
201 of the detector becomes unstable. An alternative solution is reducing the
202 thickness of the drift gap. The thinner the gap, the shorter the distance
203 between successive ionisations. For a detector with fixed operating voltages
204 and a decreased drift gap, the electric field is higher, thereby improving the

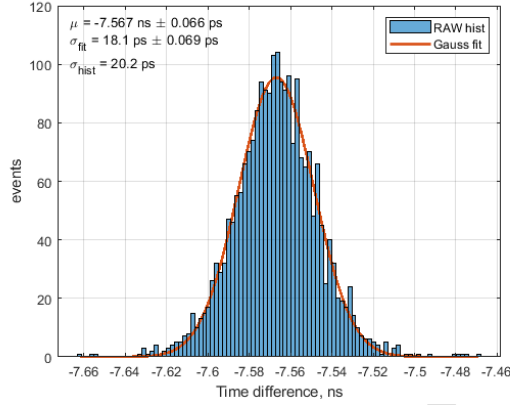


Figure 10: SAT distribution of one channel of the multipad PICOSEC while performing test beam measurements with the dedicated RF pulse amplifier cards. The voltage on the cathode was 485 V and on the anode 275 V. A geometrical cut of 4 mm diameter circle was made in the center of the pad. Time resolution of $\sigma = 20.2$ ps was measured.

205 time resolution. At the same time, the distance of the pre-amplification is
 206 shorter and the gain is smaller, ensuring a stable operation of the device at
 207 a high electric field. Fig. 11 presents a schematic design of the multipad
 208 PICOSEC with the drift gap reduced to 180 μm . The measurements of this
 209 prototype equipped with a CsI photocathode and the dedicated RF pulse
 210 amplifier cards showed a time resolution below $\sigma = 18$ ps for all measured
 211 pads [9]. An example of SAT distribution of one channel with time resolution
 212 of $\sigma = 16.7$ ps is presented in Fig. 12.

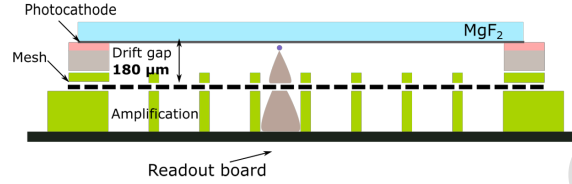


Figure 11: The PICOSEC MM detector with the drift gap reduced from 220 μm to 180 μm in order to improve time resolution [9].

213 6. Robustness of the PICOSEC Micromegas detector

214 6.1. Resistive Micromegas

215 In order to build an applicable device that can be operated in high-rate
 216 environments, the PICOSEC MM detector needs to be made more robust.
 217 The "standard" configuration of the PICOSEC prototype uses a non-resistive
 218 MM detector. Studies on resistive MM are being performed to limit the de-
 219 structive effect of discharges and achieve stable operation in intense pion
 220 beams with a resistive anode. First tests with small area (1 cm in diameter)
 221 resistive MM with anode surface resistivities of 292 $\text{k}\Omega/\square$ and CsI photo-
 222 cathode showed a time resolution of $\sigma = 24.1$ ps. Measurements with small
 223 area resistive MM of 82 $\text{M}\Omega/\square$ and Diamond Like Carbon (DLC) photocat-
 224 hode presented time resolution below $\sigma = 40$ ps, driven by the lower number
 225 of photoelectrons produced in the photocathode material. A multipad PI-
 226 COSEC with 10×10 cm^2 resistive MM of 20 $\text{M}\Omega/\square$ is being prepared to be
 227 measured in the next test beam campaign.

228 6.2. Robust photocathodes

229 The first single-pad prototype used a CsI photocathode as a converter
 230 of UV photons from the Cherenkov cone into photoelectrons. CsI is charac-

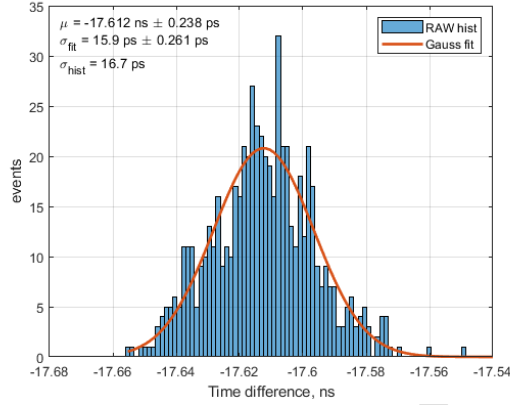


Figure 12: SAT distribution of one channel of the multipad PICOSEC while performing test beam measurements with the drift gap reduced from 220 μm to 180 μm . A geometrical cut of 4 mm diameter circle was made in the center of the pad. The voltage on the cathode was 460 V and on the anode 275 V. Time resolution of $\sigma = 16.7$ ps was measured.

231 terised by its high quantum efficiency (around 10 photoelectrons produced
 232 per minimum ionizing particle with 3 mm thick MgF_2 radiator [1]) in com-
 233 parison to other materials studied up to now. However, it can be easily
 234 damaged by ion back flow, sparks, discharges and it is sensitive to humidity.
 235 Therefore, there is a need to search for alternative photocathode materials
 236 that would be more robust. The most promising candidates are DLC, Boron
 237 Carbide (B_4C) or nanodiamonds. First measurements with the multipad
 238 PICOSEC with a DLC photocathode, a 220 μm drift gap and CIVIDEC
 239 amplifier, showed time resolution of $\sigma = 45$ ps for all measured pads [14].
 240 Additionally, comparative measurements with different thicknesses of B_4C
 241 photocathodes in small single-channel prototypes are ongoing.

242 7. Conclusions

243 Preliminary results for the $10 \times 10 \text{ cm}^2$ area PICOSEC detector demon-
244 strated a time resolution below $\sigma = 25 \text{ ps}$ per pad, showing that the excel-
245 lent timing performance of the PICOSEC detector's single-channel proof of
246 concept can be transferred to the 100-channel prototype. The best time res-
247 olution, below $\sigma = 18 \text{ ps}$, was obtained for the detector with the $180 \text{ }\mu\text{m}$ drift
248 gap, a CsI photocathode and the dedicated RF pulse amplifier cards. The
249 results made the concept more suitable for large-area experiments in need of
250 detectors with high time resolution. Developments towards applicable detec-
251 tors are ongoing. They include the improvement of stability of the detector
252 by using the multipad PICOSEC with a resistive MM and robustness studies
253 of alternative photocathode materials, e.g. DLC and B_4C . As a next step,
254 a complete readout of a 100 channel prototype with the dedicated RF pulse
255 amplifier cards and SAMPIC waveform TDC digitiser is planned. Addition-
256 ally, sealed detectors, which are clean, hermetically closed devices with high
257 gas quality, are being developed. Scaling the PICOSEC MM detector to
258 larger area by tiling $10 \times 10 \text{ cm}^2$ modules or the development of $20 \times 20 \text{ cm}^2$
259 prototype is considered to be a next step towards applicable devices.

260 Acknowledgements

261 We acknowledge the financial support of the EP R&D, CERN Strategic
262 Programme on Technologies for Future Experiments; the RD51 collaboration,
263 in the framework of RD51 common projects; the Cross-Disciplinary Program
264 on Instrumentation and Detection of CEA, the French Alternative Energies
265 and Atomic Energy Commission; the PHENIICS Doctoral School Program

266 of Université Paris-Saclay; the Fundamental Research Funds for the Central
 267 Universities of China; the Program of National Natural Science Foundation
 268 of China (grant number 11935014); the COFUND-FP-CERN-2014 program
 269 (grant number 665779); the Fundação para a Ciência e a Tecnologia (FCT),
 270 Portugal (grants IF/00410/2012 and CERN/FIS-PAR/0006/2017); the En-
 271 hanced Eurotalents program (PCOFUND-GA-2013-600382); the US CMS
 272 program under DOE contract No. DE-AC02-07CH11359.

273 Appendix A.

Table A.1: A comparison of the maximum estimated displacement in the active area for PCBs made of different materials and thicknesses given by simulations [4].

PCB mate- rial	Thickness [mm]	Displacement [μm]
FR4	3	91
	6	20
	9	10
Hybrid ceramic- FR4	2	17
	3	8
	4	4

Table A.2: Time resolution of all measured pads for the multipad PICOSEC in the "standard" configuration [3].

Pad number	Time resolution [ps]
03	24.6
06	24.1
12	25.0
13	23.9
15	22.1
16	22.9
17	24.7
18	23.0
20	23.0
26	23.9
36	23.9
41	24.0

274 References

275 [1] F. J. Iguaz, et al., for the PICOSEC Micromegas Collaboration, PI-
 276 COSEC: Charged particle timing at sub-25 picosecond precision with
 277 a Micromegas based detector, Nucl. Instrum. Methods A 903 (2018)
 278 317–325.

279 [2] S.E. Tzamarias, et al., for the PICOSEC Micromegas Collaboration,

Table A.3: Time resolution of all measured pads for the multipad PICOSEC with the custom-made amplifier cards [9].

Pad number	Time resolution [ps]
12	21.1
13	19.2
15	20.2
18	19.5
22	18.9
25	20.6
26	20.8
31	21.1
36	21.0
40	20.4

280 Timing performance of a multi-pad PICOSEC-Micromegas detector proto-
 281 type, Nucl. Instrum. Methods A 993 (2021) 165076.

282 [3] A. Utrobicic, for the PICOSEC Micromegas Collaboration, Precise tim-
 283 ing measurements with a 10x10 cm² tileable PICOSEC Micromegas de-
 284 tector module, 16th Vienna Conference on Instrumentation, 25th Febru-
 285 ary 2022.

286 [4] A. Utrobicic, for the PICOSEC Micromegas Collaboration, Me-
 287 chanical aspects of CERN GDD 10cmx10cm new PICOSEC de-

- 288 tector, RD51 Collaboration Meeting, 26th June 2020, available at
289 <https://indico.cern.ch/event/911950/contributions/3912064/> (accessed
290 on October 17th, 2022).
- 291 [5] FreeCAD open-source tools, available at <https://www.freecadweb.org>
292 (accessed on October 17th, 2022).
- 293 [6] A. Utrobicic, for the PICOSEC Micromegas Collaboration, Assembly
294 and gain uniformity measurements of a new large area PICOSEC de-
295 tector, RD51 Collaboration Meeting, 16th February 2021, available at
296 <https://indico.cern.ch/event/989298/contributions/4225012/> (accessed
297 on October 17th, 2022).
- 298 [7] CIVIDEC Instrumentation, Broadband Diamond Amplifier, available at
299 <https://cividec.at> (accessed on October 17th, 2022).
- 300 [8] C. Hoarau, et al., RF pulse amplifier for CVD-diamond particle detec-
301 tors, JINST 16 (2021) T04005.
- 302 [9] A. Utrobicic, for the PICOSEC Micromegas Collaboration, Advance-
303 ments in a large area 100 channel PICOSEC Micromegas detector
304 module, RD51 Collaboration Meeting, 14th June 2022, available at
305 <https://indico.cern.ch/event/1138814/contributions/4915978> (accessed
306 on October 17th, 2022).
- 307 [10] M. Saimpert, et al., Measurements of timing resolution of ultra-fast
308 silicon detectors with the SAMPIC waveform digitizer, Nucl. Instrum.
309 Methods A 835 (2016) 51-60.

- 310 [11] A. Kallitsopoulou, for the PICOSEC Micromegas Collaboration, First
311 Results in Signal Sharing with Multi-Pad Picosec Module Proto-
312 types, RD51 Collaboration Meeting, 16th November 2021, avail-
313 able at <https://indico.cern.ch/event/1071632/contributions/4607166/>
314 (accessed on October 17th, 2022).
- 315 [12] I. Maniatis, Research and Development of Micromegas Detectors for
316 New Physics Searches, PhD dissertation, February 2022; available
317 at <http://ikee.lib.auth.gr/record/339482/files/GRI-2022-35238.pdf> (ac-
318 cessed on October 17th, 2022).
- 319 [13] S.E. Tzamarias, et al., for the PICOSEC Micromegas Collaboration,
320 Modeling the timing characteristics of the PICOSEC Micromegas de-
321 tector, Nucl. Instrum. Methods A 993 (2021) 165049.
- 322 [14] A. Utrobicic, for the PICOSEC Micromegas Collaboration, PI-
323 COSEC Micromegas detector advancements: multi-pad de-
324 tector modules, photocathodes and detector studies, RD51
325 Collaboration Meeting, 16th November 2021, available at
326 <https://indico.cern.ch/event/1071632/contributions/4612229/> (ac-
327 cessed on October 17th, 2022).